

Jasmonate-mediated gibberellin catabolism constrains growth during herbivore attack in rice

Gaochen Jin ¹, Jinfeng Qi ², Hongyue Zu ¹, Shuting Liu ¹, Jonathan Gershenzon ³,
Yonggen Lou ¹, Ian T. Baldwin ⁴ and Ran Li ^{1,*}

- 1 State Key Laboratory of Rice Biology, Ministry of Agriculture Key Lab of Molecular Biology of Crop Pathogens and Insects, Key Laboratory of Biology of Crop Pathogens and Insects of Zhejiang Province, Institute of Insect Sciences, Zhejiang University, Hangzhou 310058, China
- 2 Department of Economic Plants and Biotechnology, Yunnan Key Laboratory for Wild Plant Resources, Kunming Institute of Botany, Chinese Academy of Sciences, Kunming 650201, China
- 3 Department of Biochemistry, Max Planck Institute for Chemical Ecology, Jena 07745, Germany
- 4 Department of Molecular Ecology, Max Planck Institute for Chemical Ecology, Jena 07745, Germany

*Author for correspondence: rli05@zju.edu.cn

The author responsible for distribution of materials integral to the findings presented in this article in accordance with the policy described in the Instructions for Authors (<https://academic.oup.com/plcell/pages/General-Instructions>) is: Ran Li (rli05@zju.edu.cn).

Abstract

Plant defense against herbivores is costly and often associated with growth repression. The phytohormone jasmonate (JA) plays a central role in prioritizing defense over growth during herbivore attack, but the underlying mechanisms remain unclear. When brown planthoppers (BPH, *Nilaparvata lugens*) attack rice (*Oryza sativa*), growth is dramatically suppressed. BPH infestation also increases inactive gibberellin (GA) levels and transcripts of GA 2-oxidase (*GA2ox*) genes, 2 (*GA2ox3* and *GA2ox7*) of which encode enzymes that catalyze the conversion of bioactive GAs to inactive GAs in vitro and in vivo. Mutation of these *GA2oxs* diminishes BPH-elicited growth restriction without affecting BPH resistance. Phytohormone profiling and transcriptome analyses revealed that *GA2ox*-mediated GA catabolism was enhanced by JA signaling. The transcript levels of *GA2ox3* and *GA2ox7* were significantly attenuated under BPH attack in JA biosynthesis (*allene oxide cyclase [aoc]*) or signaling-deficient (*myc2*) mutants. In contrast, *GA2ox3* and *GA2ox7* expression was increased in *MYC2* overexpression lines. *MYC2* directly binds to the G-boxes in the promoters of both *GA2ox* genes to regulate their expression. We conclude that JA signaling simultaneously activates defense responses and GA catabolism to rapidly optimize resource allocation in attacked plants and provides a mechanism for phytohormone crosstalk.

Introduction

Plants constantly encounter an array of different pathogens and herbivores in their natural habitats. To survive in these complicated environments, plants have evolved a set of sophisticated defense mechanisms to respond to these biotic stresses (Erb and Reymond 2019; Deng et al. 2020). However, defense activation is thought to be costly, an inference that arises from the readily observed growth restrictions that accompany defense activation (Guo et al. 2018a). This phenomenon is also known as the growth–defense trade-off, which played a central role in early theoretical considerations

of plant–herbivore interactions (Rhoades and Cates 1976; McKey 1979; Coley et al. 1985; Herms and Mattson 1992).

When attacked by herbivores, plants reallocate resources from growth to the production of defense compounds or physical barriers, which slows growth (Yang et al. 2020). Thus, plants make the allocation decision when to grow or defend, so as to optimize their fitness in the changing environment. Research into the molecular mechanisms of these growth–defense trade-offs has revealed that phytohormone signaling and the crosstalk between phytohormones play a central role (Huot et al. 2014; He et al. 2022).

IN A NUTSHELL

Background: In nature, plants frequently encounter a diverse array of insect herbivores during their lifetime. When attacked, plants activate chemical defenses, which consume resources required for plant fitness. Consequently, growth reduction is commonly associated with herbivore attack and defense activation, known as the growth–defense trade-off. The underlying mechanisms of this trade-off are commonly attributed to crosstalk among phytohormones. Jasmonate (JA) and gibberellin (GA) are defense- and growth-related phytohormones, respectively. JA signaling plays central roles in plant–herbivore interactions.

Questions: Does GA signaling participate in herbivore-elicited plant growth suppression? What is the molecular mechanism of JA–GA crosstalk in this process?

Findings: Brown planthopper (BPH) attack restricts plant growth and activates bioactive GA catabolism in rice (*Oryza sativa*). Two GA catabolism genes, *GA2ox3* and *GA2ox7*, contribute to BPH-elicited growth restriction and are upregulated by JA signaling. The core JA-responsive transcription factor MYC2 binds to the promoters of *GA2ox3* and *GA2ox7* to regulate their expression. Thus, the MYC2–*GA2ox* module regulates the growth–defense trade-off when rice is attacked by BPH.

Next steps: We will explore if other phytohormones are involved in herbivore-elicited plant growth restriction and study how they interact with JA.

Jasmonate (JA) signaling functions as a core regulator in herbivore resistance, as well as growth and development (Wasternack and Hause 2013). JA is synthesized via the octadecanoid pathway that includes a number of oxidation and reduction reactions (Chini et al. 2018; Wasternack and Feussner 2018). Jasmonyl-L-isoleucine (JA-Ile), the main bioactive form of JA in vascular plants, is perceived by JA coreceptors CORONATINE-INSENSITIVE1 (COI1) and JASMONATE ZIM domain (JAZ) proteins (Fonseca et al. 2009; Sheard et al. 2010). JAZ proteins are repressors of JA signaling that suppress various JA-responsive transcription factors (TFs), such as MYC2 (Chini et al. 2007; Thines et al. 2007). In response to herbivore attack, JA-Ile rapidly and transiently accumulates to promote the interaction between JAZs and the F-box protein, COI1, which results in the degradation of JAZs and the subsequent activation of plant defense. The underlying mechanisms of JA-mediated defense against herbivores have been broadly studied in numerous plant–herbivore systems (Erb and Reymond 2019).

JA is also known to negatively regulate plant growth. Exogenously applying JA or overexpressing JA-responsive TFs slow plant growth (Yang et al. 2012; Uji et al. 2016; Fu et al. 2022). In contrast, mutating key JA biosynthetic or signaling genes increases growth but at the expense of herbivore resistance (Yang et al. 2012; Xu et al. 2021; Wang et al. 2023). JA signaling serves as a hub in the regulation of defense–growth antagonisms. Thus, the amplification of JA signaling activated by herbivore attack is commonly associated with growth restrictions (Machado et al. 2017; Yang et al. 2020), the underlying mechanisms of which remain to be fully elucidated. Resource allocations to defense-related metabolism can slow growth due to carbon availability (Guo et al. 2018b), while JA-mediated antagonism of growth-related phytohormones (e.g. auxin and gibberellin [GA]) provides a more plausible

explanation (Hou et al. 2010; Chen et al. 2011; Yang et al. 2012). Of these, the “crosstalk” between JA and GA is best studied.

GAs are diterpene phytohormones regulating growth at diverse developmental stages, including seed germination, leaf expansion, stem elongation, and flowering (Yamaguchi 2008; Gao and Chu 2020). The major bioactive GAs, including GA_1 , GA_3 , and GA_4 , are converted from GA_{12} through oxidations by GA_{20} -, GA_3 -, and GA_{13} -oxidases (Yamaguchi 2008; He et al. 2019). Similar to JA signaling, GA signaling also engages repressor proteins (DELLAs) that interact with growth-promoting TFs, such as phytochrome interacting factors (PIFs) (de Lucas et al. 2008). Bioactive GAs bind to the GA INSENSITIVE DWARF1 (GID1) receptor and promote its interaction with DELLA, resulting in the degradation of DELLA and derepression of downstream GA-responsive genes (Sun 2011).

The JAZ proteins of JA signaling can directly interact with DELLAs (Hou et al. 2010). Activation of JA signaling leads to the degradation of JAZ, which in turn releases DELLA to suppress GA signaling and plant growth. However, the growth inhibitory effect of methyl JA (MeJA) treatments, while significantly reduced in *della* mutants, is not completely abolished, suggesting the involvement of other signaling components in JA-mediated plant growth restrictions (Hou et al. 2010; Yang et al. 2012).

Here, we examined herbivore-elicited plant growth restrictions in the monocot, rice (*Oryza sativa*). The brown planthopper (BPH, *Nilaparvata lugens*) is a notorious insect pest that continually damages rice plants in paddy fields. Our previous research revealed that JA signaling is activated in rice plants exposed to BPH attack to regulate BPH resistance (Xu et al. 2021; Wang et al. 2023). Moreover, BPH attack suppressed rice growth. We asked whether and how GA signaling participates in this process. Phytohormone profiling,

transcriptome analysis, and pharmacological approaches implicated GA2-oxidase (GA2ox)-mediated GA catabolism in BPH-induced growth suppression. The biochemical and biological functions of 2 BPH-elicited GA2oxs, GA2ox3 and GA2ox7, were examined. Growth and gene regulation assays revealed that JA signaling positively regulates BPH-elicited GA catabolism, that GA2ox3- and GA2ox7-mediated GA catabolism contributes to herbivory-elicited growth restrictions, and that the core JA-responsive TF, MYC2, directly regulates the BPH-elicited expression of GA2ox3 and GA2ox7.

Results

BPH elicitation suppresses rice growth and activates GA catabolism

To evaluate if herbivore elicitation influences rice growth, bioassays with 2 different herbivores, BPH and armyworm (AW), were performed. Ten gravid female BPH adults were allowed to attack a 4-wk-old rice seedling for 10 d; mechanically wounded and untreated plants were used as controls. Mechanical wounding (MW) mildly reduced growth. Wounded plants were diminished in stature with shorter leaf sheath (5.7% reduced) and new leaf lengths (3.6% reduced), fewer leaves (4.6% reduced), and slower growth rates (16.9% reduced). BPH attack greatly amplified these growth inhibitions (Figs. 1, A to D, and S1), and in addition, no tillers were produced in BPH-attacked plants (Fig. 1A). BPH can transmit plant viruses (e.g. *rice ragged stunt virus* [RRSV]), which could also cause the dwarf phenotype. However, PCR analysis revealed that our BPH colony was virus-free (Supplemental Fig. S2). Treating mechanical wounds with AW larval oral secretions was used to mimic AW feeding (Xu et al. 2021), and AW elicitation also suppressed rice growth (Supplemental Fig. S3, A to C), suggesting that herbivory commonly restricts growth in rice.

GAs are central growth-related phytohormones. To examine if GA signaling was altered by herbivore attack, we quantified GAs during herbivore attack. Two bioactive GAs (GA₁ and GA₄), 1 inactive GA (GA₃₄), and some precursor GAs (GA₉, GA₁₉, GA₄₄, and GA₅₃) were detected under our experimental conditions. The levels of GA₁, GA₄, and 2 precursor GAs (GA₅₃ and GA₄₄) were markedly decreased in BPH-attacked plants compared with control plants (Fig. 1, E and F). Interestingly, the levels of GA₃₄, a product of GA catabolism by 2β-hydroxylation, were much higher in BPH-attacked plants than in control plants (Figs. 1G and S4). Similarly, GA₃₄ levels were also elevated in AW-treated plants (Supplemental Fig. S3D). To determine whether herbivory-elicited growth restrictions are caused by the decrease in bioactive GAs, a bioactive GA complementation assay was conducted in which BPH-attacked plants were simultaneously supplemented with GA₄ while growth was quantified. GA₄ supplementation restored the growth of BPH-attacked plants to that of plants that had not been attacked (Supplemental Fig. S5).

To evaluate if GA biosynthesis is suppressed by herbivore attack, the expression of 2 key GA biosynthetic genes (GA3ox2 and GA20ox2) in the rice seedling stage was measured after

BPH and AW treatments (Tong et al. 2004). By reverse transcription quantitative PCR (RT-qPCR), we found that the expression of both genes did not show a clearly downregulated pattern during herbivore attack, and the transcripts of GA2ox2 were even increased in BPH-treated leaf sheath, suggesting that the biosynthesis of GA may not be directly affected by herbivore attacks (Supplemental Fig. S6).

Given that GA2ox and ELONGATED UPPERMOST INTERNODE (EUI) are important in maintaining GA homeostasis in rice by catabolizing bioactive GAs through hydroxylation (Zhu et al. 2006; Yamaguchi 2008), the expression of these deactivation genes was determined in herbivore-elicited plants. The rice genome encodes 10 GA2ox genes, and those of Clades I and II are known to function in catabolizing bioactive GAs (e.g. GA₁ and GA₄) (Hsieh et al. 2021) (Figs. 1H and S4). By mining the RNA sequencing (RNA-seq) data and RT-qPCR analysis, the GA2ox3 and GA2ox7 genes were found to be significantly upregulated in BPH and AW-elicited plants compared with control plants, while the expression of EUI did not differ (Figs. 1I and S7, A to E). GA2ox7 was highly expressed at the seedling stage and its transcripts were decreased during growth (Supplemental Fig. S7F). These results suggested that herbivory elicitation promotes the catabolism of bioactive GAs.

GA2ox3 and GA2ox7 catabolize bioactive GAs

The accumulation of inactive GAs in BPH-attacked plants might be associated with the upregulated GA2ox3 and GA2ox7. To examine if these GA2oxs are able to oxidize bioactive GAs, in vitro enzyme activity assays were conducted. GST-tagged GA2ox3 or GA2ox7 proteins were purified and incubated with GA₁ and GA₄, respectively. GST proteins with different substrates were used in control reactions. GST-GA2ox3 and GST-GA2ox7 could effectively convert GA₄ to GA₃₄ and GA₁ to GA₈ (Fig. 2, A and B).

Next, in vivo activity of GA2ox3 and GA2ox7 was evaluated by gene overexpression. As expected, GA2ox3 and GA2ox7 overexpression plants (OX3-1, -2 and OX7-1, -2) exhibited severe dwarf phenotypes (Fig. 2, C and D). Relative to GA2ox7 overexpression plants of similar age, GA2ox3 overexpression plants were much shorter (Supplemental Fig. S8). GA contents of the overexpression lines and wild-type (WT) plants were measured, and GA₁ and GA₄ levels were reduced in overexpression lines compared with WT plants (Fig. 2E). Consistent with the in vitro enzymatic assays, GA₃₄ levels were significantly increased in the OX3-1 or OX7-1 lines, and GA₈ levels were also increased in OX7-1 lines (Fig. 2F).

To further evaluate the biochemical function of these GA2oxs, the *ga2ox3*, *ga2ox7* single, and *ga2ox3 ga2ox7* double mutants were constructed by clustered regularly interspaced short palindromic repeats (CRISPR)-Cas9 (Figs. 3A and S9A). All mutations created by genome editing produced premature stop codons. To exclude transgene effects, transgene-free homozygous mutants were segregated and used for all the experiments. When planted out in paddies, *ga2ox3* (*ox3-1* and *ox3-2*) and *ga2ox3 ga2ox7* mutants (*ox3 ox7-1* and *ox3 ox7-2*) had significantly

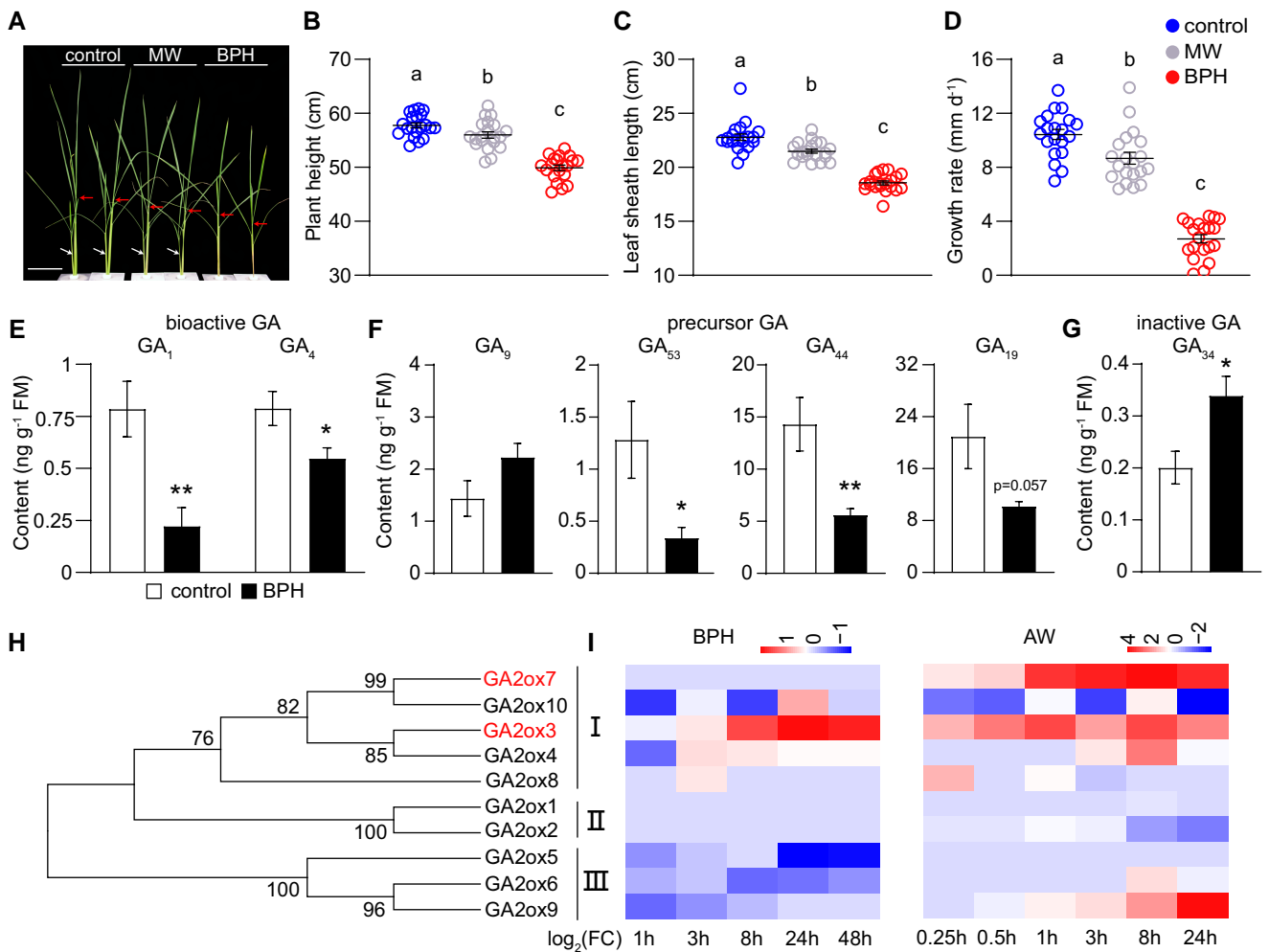


Figure 1. The growth phenotypes, GA concentrations, and expression of *GA2ox* genes in BPH-attacked and control plants. **A)** Growth phenotypes of rice seedlings under different treatments. Four-week-old rice plants were exposed to 10 female BPH adults or MW for 10 d. Nontreated plants were used as controls. White arrows indicate tillers. Red arrows indicate the top of leaf sheath. Scale bar = 10 cm. Mean height **B)**, leaf sheath length **C)**, and growth rate **D)** (\pm SE, $n = 20$) of plants under different treatments. Letters indicate significant differences among different treatments ($P < 0.05$, Duncan's multiple range test). Mean concentrations (\pm SE, $n = 6$) of bioactive GAs **E)**, precursor GAs **F)**, and inactive GAs **G)** in BPH-attacked and control plants. The GAs in each plant were measured 10 d after treatments. FM, fresh mass; asterisks indicate significant differences between BPH-attacked and control plants (* $P < 0.05$; ** $P < 0.01$; Student's t test). **H)** The phylogenetic tree analysis of *GA2ox* genes in rice. The trees were built with the maximum likelihood method. Bootstrap values (%) obtained from 1,000 replicates are shown below the branches. Roman numerals indicate different clades. The target genes are indicated by red font. **I)** Heatmap of transcription levels of *GA2ox* genes in BPH-treated leaf sheath or AW-treated leaf compared with untreated samples. Three to four biological replicates at different time intervals were used for RNA-seq analysis. The color gradient represents the relative sequence abundance; numbers in the color key indicate \log_2 fold change (FC).

longer culms compared to WT plants, while culms of *ga2ox7* mutant lines (*ox7-1* and *ox7-2*) were slightly shorter (~4% reduced) (Supplemental Fig. S9, B and C). After germination, the seedlings of *ga2ox3*, *ga2ox7*, and *ga2ox3 ga2ox7* mutants were much taller than WT plants (Supplemental Fig. S10, A and B). The GA contents in these plants were quantified. The bioactive GA_1 levels were increased in different *ga2ox* mutants compared with WT plants, while the inactive GA_{34} and GA_8 were decreased. The concentrations of bioactive GA_4 were also increased in *ga2ox3* and *ga2ox3 ga2ox7* mutants, but not in *ga2ox7* mutants (Supplemental Fig. S10, C to F). Collectively,

these results revealed that *GA2ox3* and *GA2ox7* function in the catabolism of bioactive GAs.

GA2ox3 and *GA2ox7* are involved in BPH-elicited growth restriction but not induced resistance

To evaluate the role of *GA2ox3* and *GA2ox7* in BPH-elicited growth restrictions, the growth phenotypes of *ga2ox* mutants and WT plants exposed to BPH were examined. The growth rates of *ga2ox3 ga2ox7* mutants were significantly greater than those of WT plants or single *ga2ox* mutants under BPH attack

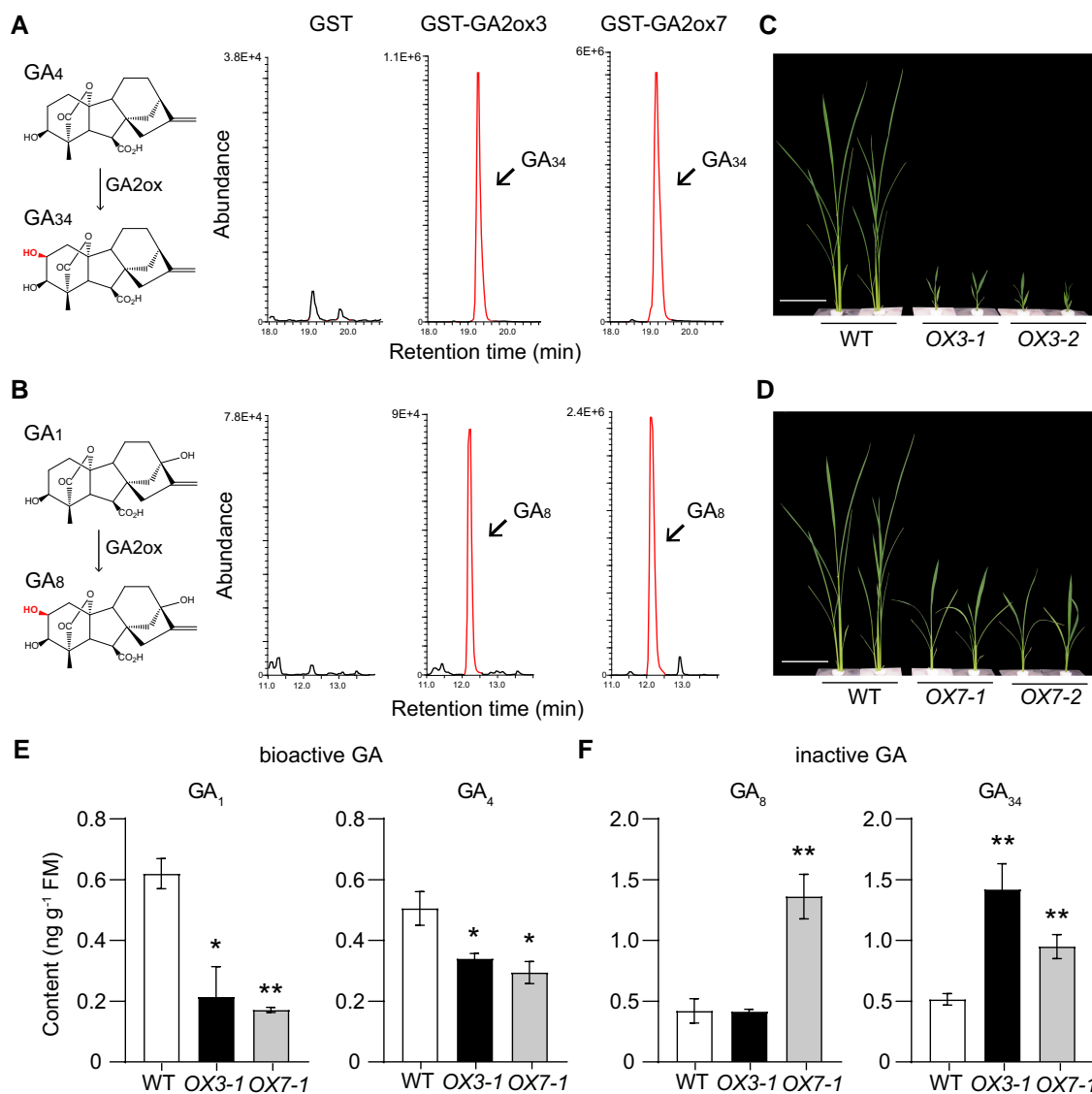


Figure 2. The *in vitro* and *in vivo* enzymatic activities of GA2ox3 and GA2ox7. Chromatograms of inactive GAs produced by the incubation of recombinant GST-fused GA2ox proteins with GA₄ **A**) or GA₁ **B**). The GST protein alone with different substrates was used as control reactions. Peaks highlighted by red lines indicate the oxidation products. **C, D**) Growth phenotype of 2 GA2ox3 overexpression lines (OX3-1 and OX3-2), 2 GA2ox7 overexpression lines (OX7-1 and OX7-2), and WT plants. Four-week-old seedlings were used. Scale bar = 10 cm. Mean concentrations (\pm SE, $n = 4$) of bioactive GAs **E**) and inactive GAs **F**) in GA2ox overexpression lines and WT plants. n , number of biological replicates; FM, fresh mass. Asterisks indicate significant differences between overexpression lines and WT plants (* $P < 0.05$; ** $P < 0.01$; Student's t test).

(Fig. 3, B and D). Accordingly, BPH elicitation reduced leaf sheath length in WT plants by 34%, while only by 24% in the *ga2ox* mutants (Fig. 3C). These results demonstrated that both GA2ox3 and GA2ox7 play a role in growth restriction during BPH attack.

To evaluate whether BPH resistance is altered in GA2ox mutants, BPH performance assays were conducted on these plants. Previous research revealed that mutating *allene oxide cyclase* (AOC) and MYC2 genes by CRISPR-Cas9 significantly attenuated JA biosynthesis and signaling, respectively, and plant resistance to BPH (Xu et al. 2021). Here, the *myc2-5* mutant was used as a positive control. The hatching rate of BPH eggs was significantly increased in *myc2-5* compared with WT

plants, and the hatching duration of BPH eggs on *myc2-5* was shorter than on WT plants (Supplemental Fig. S11, A to C). However, the hatching rate, hatching duration of BPH eggs, and the number of eggs laid by per female per day did not differ among different *ga2ox* single or double mutants and WT plants (Supplemental Fig. S11, D to F). To further validate these observations, a BPH-elicited rice survival assay was conducted. Consistent with the hatching assay, the *myc2-5* lines were more severely damaged by BPH than WT plants, while *ga2ox* mutants and WT plants did not differ (Supplemental Fig. S11, G to J). Collectively, these results suggested GA2ox3 and GA2ox7 are not involved in resistance to BPH.

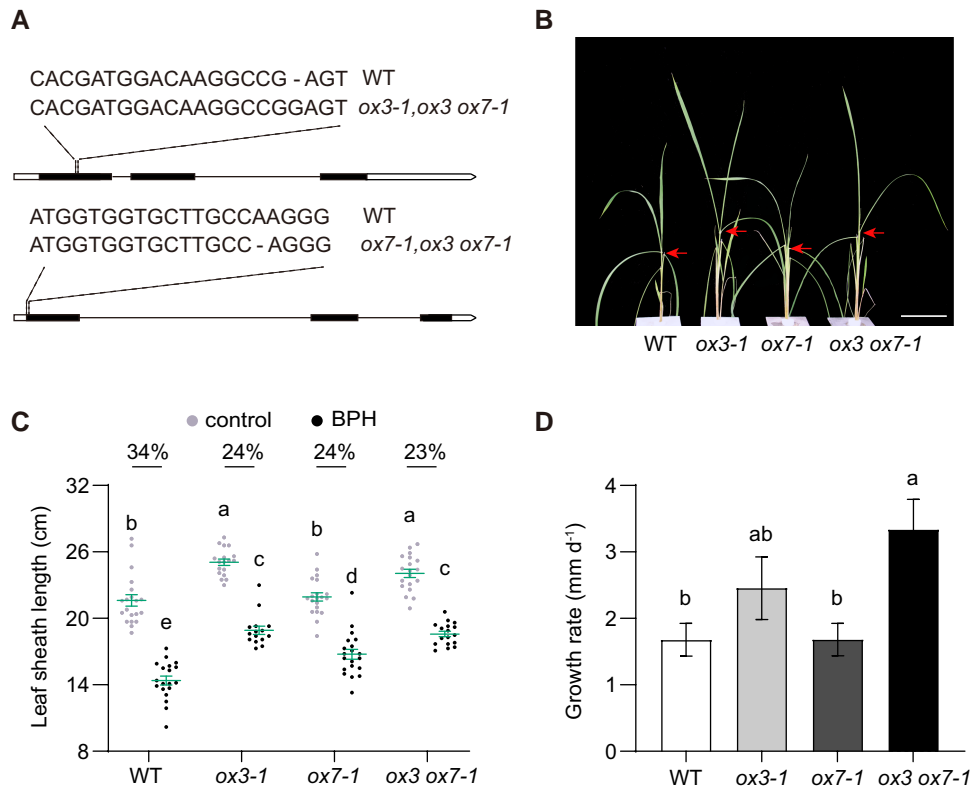


Figure 3. The BPH-elicited growth phenotype of *ga2ox* mutants and WT plants. **A)** Mutation of *GA2ox* genes by CRISPR/Cas9. Target sequences of sgRNA were listed. *ox3-1*, *GA2ox3* mutant; *ox7-1*, *GA2ox7* mutant; *ox3 ox7-1*, *GA2ox3* and *GA2ox7* double mutant. **B)** Growth phenotypes of *GA2ox* mutants and WT plants exposed to BPH; red arrows indicate the top of leaf sheath; scale bar = 10 cm. Mean leaf sheath lengths **C)** and growth rates **D)** (\pm SE, $n = 15$ to 20) of *GA2ox* mutants and WT plants under different treatments. n , number of biological replicates. The growth–restriction ratios of leaf sheath caused by BPH attack (on the top of the scatter plot) were calculated by length decrements. Letters indicate significant differences among different plants ($P < 0.05$, Duncan’s multiple range test).

JA signaling regulates herbivore-induced GA catabolism

Herbivore attack is known to rapidly activate JA-mediated defense responses in plants (Erb and Reymond 2019). The concentrations of jasmonic acid and JA-Ile were much higher in BPH-elicited plants compared with unelicited controls (Fig. 4, A and B). Given that JA signaling plays a central role in prioritizing defense over growth, BPH-elicited GA catabolism may be regulated by JA. To test this hypothesis, MeJA treatments and JA-deficient rice lines were employed. The levels of *GA2ox3* and *GA2ox7* transcripts were significantly up-regulated in MeJA-treated plants compared with control plants (Figs. 4C and S12). Accordingly, the levels of GA_{34} , the product of *GA2ox3* and *GA2ox7* activity, were also increased with MeJA treatment (Fig. 4D).

Next, transcript levels of *GA2ox3* and *GA2ox7* in BPH-elicited JA mutants were examined. Relative to WT plants, *aoc* and *myc2* mutants are taller with longer roots (Supplemental Fig. S13), implying that functional JA signaling slows growth. *GA2ox3* and *GA2ox7* transcript levels were significantly lower in *aoc* or *myc2* mutants than in WT plants in response to BPH attack (Fig. 4, E and F). Given that MYC2 is the master regulator TF in JA signaling, lines overexpressing

Flag-tagged MYC2 were constructed (*oeMYC2*). Flag-GFP overexpression lines (*oeGFP*) were used as controls (Supplemental Fig. S14, A and B). In contrast to the JA mutants *aoc* and *myc2*, *oeMYC2* lines were stunted in their growth (Figs. 4G and S14, C and D). Moreover, levels of *GA2ox3* and *GA2ox7* transcripts were constitutively higher in *oeMYC2* lines than in control plants (Fig. 4H). The levels of JA and JA-Ile were constitutively accumulated in *oeMYC2* lines at seedling and tillering stages, suggesting that JA-mediated responses are constitutively activated in *oeMYC2* (Supplemental Fig. S15, A and B). As expected, the bioactive GA_4 levels were decreased in *oeMYC2* compared with control plants, while the concentrations of inactive GA_{34} were increased (Supplemental Fig. S15, C to F). Collectively, these data are consistent with the hypothesis that JA signaling mediates BPH-elicited GA catabolism.

To further evaluate the role of JA in growth restrictions during BPH attack, the BPH-elicited GA catabolism and growth phenotype of the *myc2* mutant were examined. In contrast to *oeMYC2* lines, *myc2* mutants accumulated lower levels of GA_{34} but higher levels of GA_4 than WT plants in response to BPH attack (Figs. 4I and S16). Although the length of leaf sheaths did not differ between *myc2-5* and WT plants

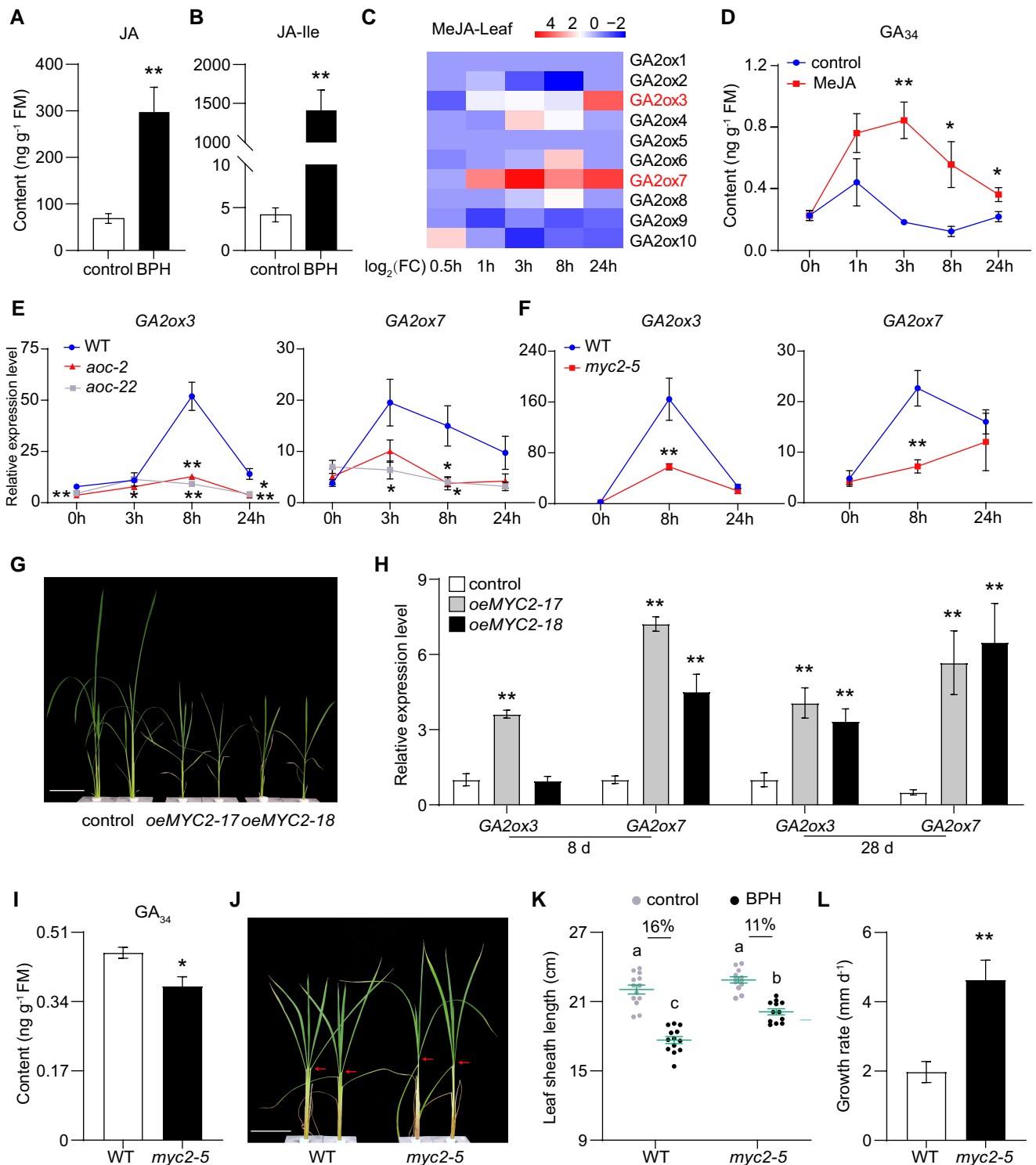


Figure 4. The association between herbivore-induced JA signaling and GA catabolism. Mean jasmonic acid **A**) and JA-Ile **B**) concentrations (\pm SE, $n = 6$) in BPH-attacked and control plants. n , number of biological replicates. **C**) Heatmap of transcript levels of *GA2ox* genes in MeJA-treated samples compared with control samples. Three biological replicates at different time intervals were used for RNA-seq analysis. The color gradient represents the relative sequence abundance; numbers in the color key indicate log₂ fold change (FC). The target genes are indicated by red font. **D**) Mean concentrations (\pm SE, $n = 6$) of GA₃₄ in MeJA-treated and control plants. FM, fresh mass. Asterisks indicate significant differences between treated and control plants (* $P < 0.05$; ** $P < 0.01$; Student's t test). Mean transcript abundances (\pm SE, $n = 5$ or 6) of *GA2ox3* and *GA2ox7* genes in *aoc* **E**) or *myc2* **F**) mutants and WT plants under BPH treatments. **G**) Growth phenotypes of *MYC2* (*oeMYC2-17*, -18) and *GFP* (control) overexpression lines. Four-week-old seedlings were used. Scale bar = 10 cm. **H**) Mean transcript abundances (\pm SE, $n = 6$) of *GA2ox3* and *GA2ox7* genes in *oeMYC2* and control plants at different developmental stages. **I**) Mean concentrations (\pm SE, $n = 6$) of GA₃₄ in *myc2-5* and WT plants under BPH treatments. **J**) The performance of *myc2* mutant and WT plants exposed to BPH. Pictures were taken 12 d after treatment. Red arrows indicate the top of leaf sheath.

(continued)

under normal conditions, those of *myc2-5* were longer than those of WT plants exposed to BPH (Fig. 4, J and K). Accordingly, the growth rates of *myc2-5* mutants were significantly faster than those of WT plants under BPH attack (Fig. 4L), demonstrating that BPH-elicited growth restriction was diminished in *myc2* mutants.

MYC2 directly regulates the expression of GA2ox3 and GA2ox7

To clarify the transcriptional regulation mechanism of herbivore-associated GA2oxs, the cis-elements in 2-kb promoter regions of GA2ox3 and GA2ox7 were screened. Interestingly, many G-box or G-box-like motifs were identified (Fig. 5A and Supplemental Data Set 1), which are binding sites of bHLH TFs, such as those of the MYC2 group (MYC2, MYC3, and MYC4) (Fernández-Calvo et al. 2011; Kazan and Manners 2013; Zander et al. 2020). Given the roles of MYC2 in BPH-elicited expression of GA2oxs and growth restriction, MYC2 may directly regulate the expression of these genes.

To test this hypothesis, in vivo transcription activation assays were performed. The 2-kb GA2ox3 or GA2ox7 promoter:GUS was used as a reporter and myc-tagged MYC2 or myc-SV40 nuclear localization sequences (NLS) were used as effectors (Fig. 5B). The indicated reporter and effector constructs were transiently expressed in leaf cells of *Nicotiana benthamiana*. GUS activities were significantly higher in *myc-MYC2*-expressing leaves than in *myc-SV40* NLS-expressing leaves (Fig. 5, C and D), suggesting MYC2 could activate the expression of GA2ox3 and GA2ox7. Electrophoretic mobility shift assays (EMSAs) were conducted to identify the potential binding motifs of MYC2. His-tagged MYC2 protein was purified from *Escherichia coli* and a total of 9 different G-box motifs were screened. MYC2 protein can directly bind to G-box (motif #1, CACGTG)- and 2 G-box-like motifs (#2, CATGTG, and #8, CATATG)-containing probes from different promoters (Fig. 5E). Furthermore, mutation of these motifs abolished MYC2 binding. DNA binding specificity was further confirmed by a competition experiment using excess unlabeled cold probes which led to the disappearance of the labeled DNA/protein complex (Fig. 5E). To confirm these interactions in vivo, the chromatin immunoprecipitation (ChIP) assays were performed. As expected, the DNA regions containing G-box (1#) or G-box-like (2# and 8#) motifs were enriched in Flag-MYC2 precipitated samples compared to Flag-GFP precipitated ones (Fig. 5F). Taken together, these results indicated that MYC2 could directly bind to GA2ox3 and GA2ox7 promoters and activate their expression.

Figure 4. (Continued)

Scale bar = 10 cm. Mean lengths of leaf sheath (K) and growth rates (L) (\pm SE, $n = 20$) of *myc2* mutants and WT plants under different treatments. Asterisks indicate significant differences in *oeMYC2* or *myc2-5* compared to control plants (* $P < 0.05$; ** $P < 0.01$; Student's *t* test). Letters indicate significant differences among different plants ($P < 0.05$, Duncan's multiple range test). For RT-qPCR analysis, the transcription level of each gene was normalized with the rice *Ubiquitin* gene. The lowest transcription level of each gene in all samples was set as "1."

To further evaluate the involvement of MYC2 and GA2ox in the same GA signaling pathway, we performed GA complementation assays using MYC2, GA2ox3, and GA2ox7 overexpression lines. All 3 overexpression lines exhibit stunted growth due to the activated GA catabolism. Exogenous application of bioactive GA could restore the growth of *oeMYC2* and OX7 to greater than that of WT, while partially restoring the growth of OX3 (Supplemental Fig. S17), suggesting that the MYC2-GA2ox module plays a role in GA catabolism.

The JAZ-DELLA module also regulates BPH-elicited growth restrictions, but not through GA2oxs

The GA signaling repressor, DELLA protein, has also been implicated in JA-mediated growth restriction (Yang et al. 2012). The Arabidopsis (*Arabidopsis thaliana*) genome encodes 5 DELLA genes, while tomato (*Solanum lycopersicum*) and rice only have 1. DELLA is known to interact with JAZ proteins in Arabidopsis and tomato (Hou et al. 2010; Panda et al. 2022). In Arabidopsis, AtJAZ3 and AtJAZ9 could interact with DELLA in yeast (*Saccharomyces cerevisiae*) (Hou et al. 2010). Yeast 2-hybrid assays revealed that rice JAZ3, JAZ4, and JAZ9, the orthologs of Arabidopsis AtJAZ3 and AtJAZ9, also strongly interact with DELLA (Supplemental Figs. S18 and 6A). In Arabidopsis, MYC2 could also interact with DELLA (Hong et al. 2012). However, we did not detect these interactions in rice by in vitro pull-down and in vivo bimolecular fluorescence complementation (BiFC) assays (Supplemental Fig. S19).

The growth rates of the *della* mutant (*slr1*) were greater than that of WT plants (ZH11) exposed to BPH (Fig. 6, B and D). Moreover, the BPH inhibition of leaf sheath lengths was attenuated in *slr1* mutants (10%) compared with WT plants (20%) (Fig. 6C), suggesting that DELLA is also involved in BPH-elicited growth restrictions. However, the transcript levels of GA2ox3 and GA2ox7 were increased in BPH-attacked *slr1* mutants compared with WT plants, which is contrast to that in *myc2* mutants (Fig. 6, E and F). These results suggest that DELLA and MYC2 regulate BPH-elicited expression of GA2oxs in different ways that require future study.

Discussion

Defense and growth trade-offs are commonly thought to be regulated by phytohormonal "crosstalk" (Huot et al. 2014), but the mechanisms of these interactions are poorly understood. Here we provide 3 lines of evidence that JA-mediated GA catabolism is partially responsible for BPH-elicited growth inhibition in rice. First, GA2ox-mediated GA

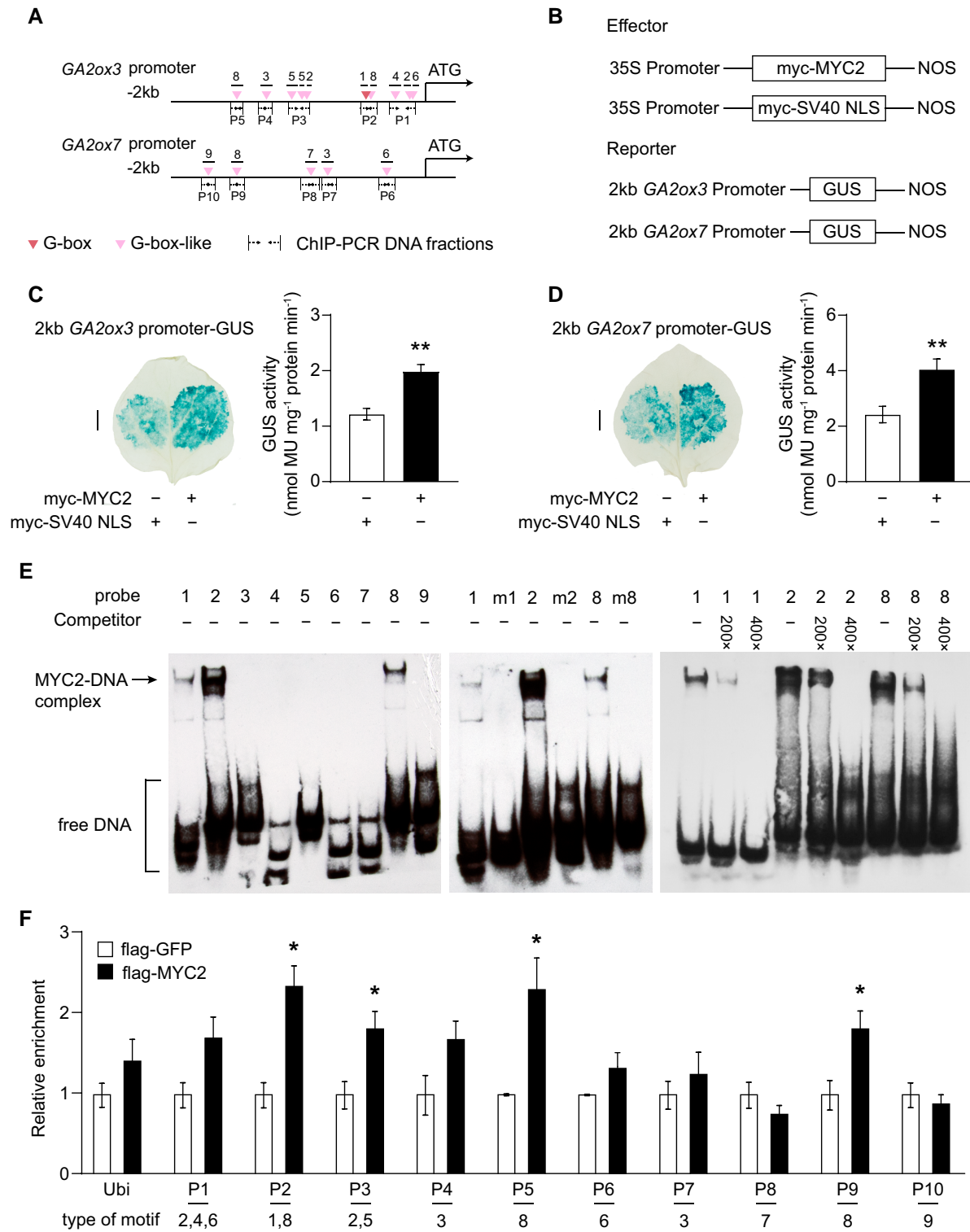


Figure 5. The transcriptional regulation between MYC2 and GA2ox genes. **A**) Schematic of the GA2ox3 and GA2ox7 2-kb promoter. The triangles represent G-box or G-box-like motifs and the numbers above represent putative types (see details in [Supplemental Data Set 1](#)). The zones (P1 to P10) below indicate fragments amplified in ChIP assays. **B**) Constructs of effector and reporter used for transcriptional activation assays. SV40 NLS was used as control. Transcriptional activation assays of GA2ox3 **C**) and GA2ox7 **D**). Leaves of *N. benthamiana* were agroinfiltrated with the indicated reporter and effector constructs. Scale bar = 1 cm. The GUS activity (\pm SE, $n = 7$ to 8) of infiltrated leaf cells was quantified after 48 h. n , number of biological replicates. Asterisks indicate significant differences between different treatments (** $P < 0.01$; Student's t test). **E**) DNA binding ability of MYC2 was analyzed by EMSA. Probes 1 to 9 containing G-box or G-box-like motifs were designed according to **A**). The recombinant His-tagged MYC2 protein was purified and used in the assays. The G-box or G-box-like motifs in the probes were mutated (m). Competition experiments were performed using unlabeled probes as competitors in a different fold molar excess. **F**) Mean enrichment (\pm SE, $n = 3$) of GA2ox3 and GA2ox7

(continued)

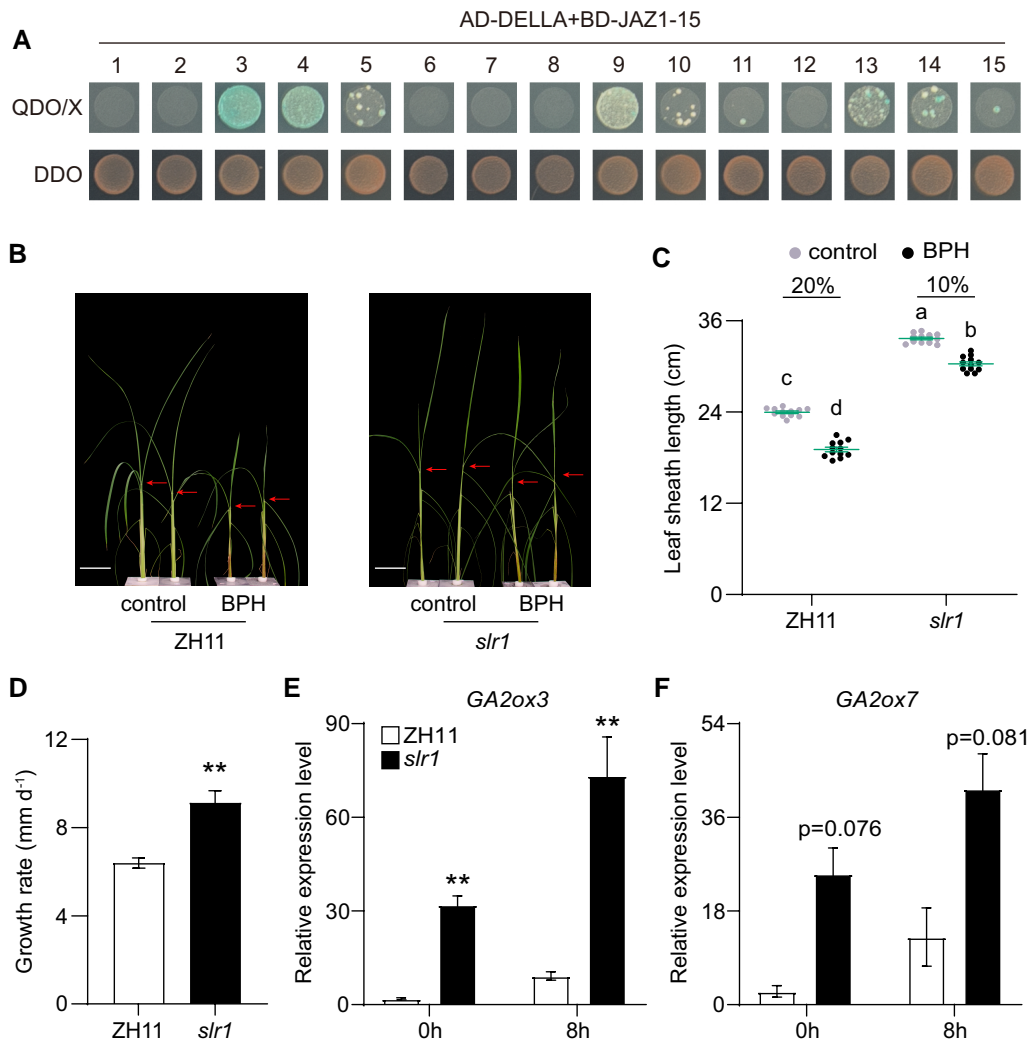


Figure 6. The JAZ–DELLA module in BPH-elicited growth restrictions and *GA2oxs* transcript levels. **A)** BD–JAZs and AD–DELLA were cotransformed into yeast strain Y2H–Gold. Transformants were grown on DDO (double dropout supplements, SD–Leu/–Trp) and QDO (quadruple dropout supplements, SD–Ade/–His/–Leu/–Trp) plates. **B)** Growth phenotype of *slr1* mutants (DELLA mutation) and WT plants (ZH11) exposed to BPH. Pictures were taken 12 d after treatment. Red arrows indicate the top of leaf sheath. Scale bar = 10 cm. Mean lengths of leaf sheath **C)** and growth rate **D)** (\pm SE, $n = 12$) of *slr1* mutants and WT plants under different treatments. n , number of biological replicates. The growth–restriction ratios of leaf sheaths caused by BPH attack (on the top of the scatter plot) were calculated by length decrements. Letters indicate significant differences among different plants ($P < 0.05$, Duncan’s multiple range test). Mean transcript levels (\pm SE, $n = 5$) of *GA2ox3* **E)** and *GA2ox7* **F)** genes in *slr1* and WT plants. The transcription level of each gene was normalized with the rice *Ubiquitin* gene. The lowest transcription level of each gene in all samples was set as “1.” Asterisks indicate significant differences in *slr1* compared to control plants (** $P < 0.01$; Student’s *t* test).

catabolism was increased in BPH-attacked plants and the elicited growth restrictions could be reversed by supplementing plants with bioactive GA. Second, 2 BPH-elicited *GA2oxs*, *GA2ox3* and *GA2ox7*, were shown to catabolize bioactive GAs and mutations of both genes attenuated the

BPH-elicited growth restrictions. Third, MeJA treatment induced similar *GA2ox*-mediated GA catabolism and the expression of *GA2ox3* and *GA2ox7* were directly regulated by the core JA-responsive TF, MYC2. Mutation of MYC2 also diminished BPH-elicited GA catabolism and growth

Figure 5. (Continued)

chromatin fragments in Flag–MYC2 precipitated samples compared to Flag–GFP precipitated ones. The 35S:Flag–MYC2 and 35S:Flag–GFP transgenic plants were used. 35S, *Cauliflower Mosaic Virus* 35S promoter. Seeds of these plants were germinated and grown in the 1/2 agar plate containing Hygromycin B. Five-day-old seedlings were used for ChIP assay. An *Ubiquitin* fragment was amplified as the negative control. The enrichment of each fragment was normalized with the rice *Actin* gene. The relative enrichment of each fragment in Flag–GFP precipitated sample was set as “1.” The fragments of P1 to P10 were indicated in **A)**. Asterisks indicate significant differences between different treatments (* $P < 0.05$; Student’s *t* test).

restrictions. This MYC2–GA2ox regulatory module was shown to function differentially from the JAZ–DELLA module which also contributes to BPH-elicited growth restrictions. These 3 lines of evidence provide a granular mechanistic description of an herbivory-elicited phytohormonal crosstalk, and in the following, we discuss this mechanism in the context of other well-characterized crosstalks.

Of JA–GA crosstalks, the JAZ–DELLA module has received considerable attention (Hou et al. 2010; Panda et al. 2022). In the current work, a single DELLA protein was shown to strongly interact with JAZ3, JAZ4, and JAZ9 in yeast (Fig. 6A). Previous work had shown that DELLA functions in JA-mediated growth restrictions (Yang et al. 2012). As expected, the BPH-elicited growth restrictions were attenuated in the rice *della* mutant compared to WT plants, partially phenocopying the growth response of the *myc2* mutant; however, the response of the GA2ox genes differed in the 2 mutants, implying that the JA–GA2ox and JA–DELLA regulatory modules function differentially in BPH-elicited growth restrictions. High levels of GA signaling are known to suppress GA production by promoting the expression of the GA-deactivation gene, GA2ox, to maintain GA homeostasis (Yamaguchi 2008). The high basal expression of GA2oxs in the *della* mutant may be regulated by a negative feedback loop in the GA pathway. By mining Arabidopsis ChIP-seq data of MYC2/3 and transcriptome data of *myc2* mutant (Zander et al. 2020), both MYC2 and MYC3 can directly bind to the promoters of *AtGA2ox2*, an ortholog of rice GA2ox3 and GA2ox7 in Arabidopsis. Furthermore, the expression of *AtGA2ox2* was upregulated by JA treatment and decreased in *myc2* mutants compared with WT plants (Supplemental Fig. S20), suggesting MYC2/3 could also regulate the transcription of *AtGA2ox2* in Arabidopsis. The MYC2–GA2ox regulatory module seems to be conserved in plants, but this should be confirmed by further investigation.

In addition to the GA pathway, MYC2 is also known to mediate growth responses by interacting with other growth-related phytohormones (Guo et al. 2018a). For instance, MYC2 inhibits root growth by antagonizing auxin signaling, by directly repressing the auxin-responsive TFs, *PLETHORA1* (*PLT1*) and *PLT2*, both of which promote cell proliferation in root meristems (Chen et al. 2011). We observed that BPH attack also attenuated rice tillering, but GA complementation did not restore tiller production. Collectively, these results suggest that other phytohormones are also involved in JA-mediated growth restriction and future studies of how the JAZ–MYC2 module interacts with other hormonal signaling are needed.

GA2ox is encoded by a gene family in seed plants with a great diversity of expression profiles. Some genes are expressed in early developmental stages, while others are expressed later, and some are responsive to abiotic stresses (Lo et al. 2008; Li et al. 2019). Here, BPH attack of leaf sheaths and AW treatment of leaves both increased GA2ox3 expression. However, GA2ox7 transcripts were dramatically upregulated in AW-treated leaves, but only mildly increased in

BPH-attacked leaf sheaths (Figs. 1I and S7), suggesting GA2ox7 likely functions mainly in leaves, while GA2ox3 may play roles throughout the entire plant.

Based on protein sequence similarity, GA2oxs are classified into 3 clades: members of Clades I and II catalyze reaction with C₁₉-GAs, including all bioactive GAs, while Clade III proteins catalyze reaction with C₂₀-GAs. Altering the expression of GA2ox3 or GA2ox7 resulted in different growth phenotypes. GA2ox3 overexpression lines were more stunted than GA3ox7 overexpression lines, consistent with previous studies (Hsieh et al. 2021). Furthermore, mutation of a single GA2ox3 was sufficient to increase plant growth, suggesting a stronger role for GA2ox3 compared with GA2ox7, which may reflect the importance of variations in 4 conserved amino acids between GA2ox3 and GA2ox7 (Hsieh et al. 2021). Mutation of GA2ox7 did not significantly affect rice growth at the tillering and mature grain stage, but increased growth at the seeding stage (Figs. 3B, S9, and S10). This is consistent with the expression of GA2ox7 during growth (Supplemental Fig. S7F).

Although the BPH-elicited growth rate did not differ between WT and the *ga2ox7* mutant, the growth–restriction ratios of leaf sheaths caused by BPH attack were lower in *ga2ox7* than in WT. Moreover, the BPH-elicited growth rate of the *ga2ox3 ga2ox7* double mutant was higher than that of the *ga2ox3* or *ga2ox7* single mutant, suggesting that these genes play redundant roles in JA-mediated rice growth. It is worth noting that the expression of other Clade I GA2oxs, GA2ox4, 8, and 10, were also mildly induced by herbivory and MeJA treatments. Mutations of individual genes and the entire Clade I would be required to evaluate if these GA2oxs are also involved in JA-mediated growth.

The crosstalk between phytohormones and other signaling pathways is a common mechanism in regulating many physiological processes in plants. Some of these interactions are synergistic while some of them are antagonistic. For instance, growth- and defense-related signaling usually antagonize each other. Photoreceptor B-mediated light signaling suppresses plant defense by activating sulfotransferase-mediated JA catabolism under shade conditions (Fernández-Milmanda et al. 2020). Our results also revealed that BPH-elicited JA restricts rice growth by promoting GA2ox-mediated GA catabolism. Thus, it seems that the induction of phytohormone degradation (PHD) may represent a more general mechanism of antagonistic “crosstalk.” It has been reported that 3 JA-responsive NAC TFs could activate salicylic acid (SA) methyltransferase-mediated SA catabolism to suppress Arabidopsis antibacterial defense during *Pseudomonas syringae* infection (Zheng et al. 2012). A recent study also found that strigolactones could promote the catabolism of cytokinins to regulate shoot architecture in rice (Duan et al. 2019).

In summary, this study revealed a mechanism for the JA-mediated growth and defense trade-off. The core JA-responsive TF, MYC2, binds to the promoters of GA catabolism genes, GA2ox3 and GA2ox7, and subsequently

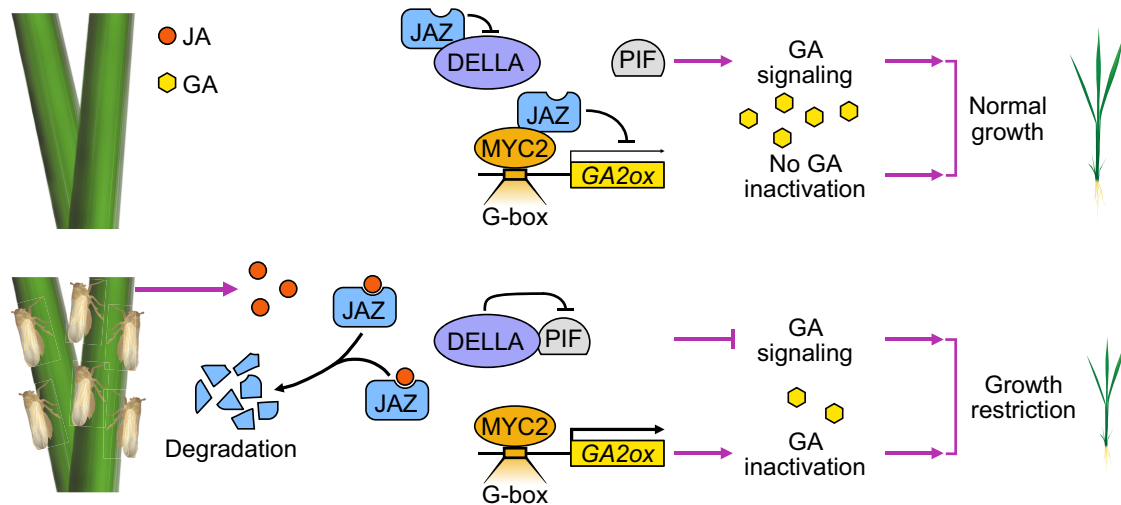


Figure 7. A working model of JA-mediated growth restriction during herbivore attack. Herbivore-elicited JA signaling suppresses plant growth by interacting with GA pathway. Both MYC2–GA2ox and JAZ–DELLA modules are involved in this process. JAZ and DELLA are suppressors of the JA and GA signaling pathways, respectively. PIF, phytochrome interacting factor.

regulates their expression. In unattacked plants, the JAZ proteins of JA signaling suppress MYC2 and the GA signaling repressor, DELLA, to sustain rapid growth without activating plant defense. In response to herbivore attack, JA biosynthesis is rapidly activated and the bioactive JA-Ile binds to JA coreceptors, which leads to the degradation of JAZs and the release of MYC2 and DELLA. JA-mediated plant defense against herbivores is activated by MYC2. Meanwhile, MYC2 reduces bioactive GAs by activating GA2ox-mediated GA catabolism, and DELLA suppresses the GA-responsive TFs (e.g. PIF) and downstream GA responses. In this way, both pathways coordinate their outputs to mediate growth restrictions (Fig. 7).

Overall, our results provide important mechanistic insights into how phytohormonal crosstalk mediates the growth and defense trade-off. Such understanding could be valuable for plant breeding strategies that seek to maximize yield without compromising resistance. Our observation that the growth-promoting mutations in *GA2ox3* and *GA2ox7* genes did not alter rice resistance to BPH needs to be verified in field trials over several growing seasons, but they suggest that it is possible to uncouple the growth and defense trade-off to produce plants with both strong defense and uncompromised growth (Guo et al. 2018a; He et al. 2022).

Materials and methods

Plant materials and growth conditions

O. sativa japonica variety, Xiushui 11 (XS11), was used as the WT. Rice seeds were germinated in plastic petri dishes with water in an illuminated incubator at 26 to 28 °C under 16 h of light (Light emitting diode [LED] light with an intensity of $\sim 100 \mu\text{mol m}^{-2} \text{s}^{-1}$). Seven-day-old seedlings were transferred to hydroponic cultivation as described previously

(Fu et al. 2022). Plants were grown in a growth chamber under 14-h light (28 °C) and 10-h dark (26 °C) photoperiod, with a light intensity of $\sim 140 \mu\text{mol m}^{-2} \text{s}^{-1}$ (LED light) and 60% relative humidity. Three-week-old rice plants were used for experiments. Seeds of *N. benthamiana* were germinated on soil and seedlings were grown in the same growth chamber as above. Four-week-old *N. benthamiana* plants were used for experiments.

Plant growth inhibition assays

For BPH treatments, plants were infested with 10 gravid female adults confined in a glass cage (diameter 4 cm and height 8 cm, with 24 holes, diameter 0.8 mm). For MW treatments, the leaf sheath was pricked with a microneedle (diameter 0.45 mm) 400 times every 24 h. Plants with an empty cage were used as controls. Plant height and leaf sheath length (attached to the uppermost expanded leaf) of each seedling were measured before and after treatments. The growth rate was determined from height increment. For AW (*Mythimna separata*) treatments, 20 μL AW larval oral secretions were rubbed into freshly produced puncture wounds created by rolling a fabric pattern wheel across the lamina of a new leaf every 48 h. Untreated plants were used as controls. For GA complementation assays, plants were transferred to hydroponic cultivation containing 0.5 μM GA₄. Plants in hydroponic cultivation with solvent were used as controls. Each plant was infested with 10 gravid female adults as described above. Ten days later, plant height and leaf sheath length of each seedling were measured before and after treatment.

Plant sample collections

BPH treatments were conducted as described above with 15 gravid female adults. The 2 outermost leaf sheaths and their

associated leaves were collected at the indicated time points. For AW treatments, the youngest fully expanded leaf was treated as described above. The leaves from untreated plants were used as controls. Samples were collected at the indicated time points. For MeJA treatments, plants were transferred to hydroponic cultivation containing 100 μM MeJA. Plants in hydroponic cultivation with solvent were used as controls. The first fully expanded leaves were collected at the indicated time points.

Phylogenetic analysis

Sequences were aligned with CLUSTALW, and the trees were built with the maximum likelihood method in MEGA11. Bootstrap values (%) obtained from 1,000 replicates is taken to represent the evolutionary history.

Phytohormone analyses

For JA analysis, \sim 150 mg of leaf material (precise mass was recorded) was ground and extracted in 1 mL of ethyl acetate containing the internal standards (10 ng of D₆-JA and 8 ng of D₆-JA-Ile). Extracts were analyzed by LCMS-8040 (Shimadzu) as described previously (Fu et al. 2022).

For GA analysis, about 150 mg material was ground and extracted with 4 mL acidified MeOH (MeOH:H₂O:HCOOH 15:4:1 [*v:v:v*]) containing the internal standard (5 ng of D₂-GA₄ and 5 ng of D₂-GA₁). Extracts were analyzed by LCMS-8040 as described previously (Liu et al. 2019). GA₄, GA₃₄, and GA₉ were quantified using the internal standard D₂-GA₄, and GA₁, GA₈, GA₁₉, GA₄₄, and GA₅₃ with D₂-GA₁.

Transcriptome analysis

Total RNA isolated from control and AW or MeJA-treated leaf sheaths of different plants were used for RNA-seq. RNA-seq was performed by the Novogene company. Three biological replicates were used for each line and treatment. Adaptor sequences and low-quality reads were removed using FASTP (Chen et al. 2018). Clean reads were mapped to the rice reference genome (http://rice.plantbiology.msu.edu/pub/data/Eukaryotic_Projects/o_sativa/annotation_dbs/pseudomolecules/) using HISAT2 (Kim et al. 2015). The read counts were obtained and normalized (transcripts per million [TPM]) by STRINGTIE (Pertea et al. 2015).

Production and purification of recombinant proteins

The full-length ORF of GA2ox3 and GA2ox7 without stop codon was PCR-amplified and introduced into the pDEST15 (Thermo Fisher) vector. The full-length ORF of MYC2 was amplified and introduced into the pET-28b (Novagen) and pGEX-4T-1 vector. The primers used for PCR amplification are listed in Supplemental Data Set 2. The GA2ox3- and GA2ox7-related constructs were transformed into *E. coli* BL21 (DE3), while MYC2-related constructs were transformed into *E. coli* Rosetta (DE3). The overnight culture containing different constructs was transferred to a 500-mL LB medium with 50 mg L⁻¹ kanamycin and incubated to OD₆₀₀ 0.4 to 0.5 at 37 °C. The expression was induced by

adding 0.4 mM isopropyl- β -thiogalactopyranoside (IPTG) for 3 h at 37 °C. Cells were collected and the recombinant protein was purified using GST or His Trap (GE Healthcare) according to manufacturer's instructions.

Enzymatic activity assay

The reaction mixtures (150 μL) contained 10 μg recombinant GA2ox, 50 μM GA₁ or GA₄, 5 mM DTT, 13.3 mM α -ketoglutarate, 13.3 mM ascorbate, 0.67 mM iron(II), and 5 μg μL^{-1} BSA in 50 mM Tris-HCl (pH 8.0). The reaction mixture was incubated in an incubator at 30 °C for 1 h and stopped by adding 1/5 volume of 1 M HCl before extraction with 180 mL of ethyl acetate. After centrifugation at 14,000 $\times g$ for 1 min, the upper organic phase was dried by a Concentrator Plus (Eppendorf) and dissolved in 200 μL methanol before LC-MS/MS analysis.

Generation and characterization of transgenic plants

To generate GA2ox3, GA2ox7, and double gene-deficient lines, the target sequence of GA2ox3 and GA2ox7 genes was introduced into pLYsgRNA-OsU3 and pLYsgRNA-OsU6b to yield rice U3/U6b promoter-driven single-guide RNA (sgRNA), respectively. The sgRNA expression cassette containing single GA2ox or both GA2oxs was then introduced into plant CRISPR-Cas9 binary vector pYLCRISPR/Cas9Pubi-H (Ma et al. 2015). The T-DNA was inserted into rice variety, XS11, using EHA105 *Agrobacterium tumefaciens*-mediated transformation. Plants with mutations but lacking the T-DNA were screened by target DNA sequencing and hygromycin gene identification.

To generate overexpression lines, the full-length ORFs of GA2ox3 or GA2ox7 were ligated into vector pCAMBIA1301 (Cambia) under control of the CaMV 35S promoter. The full-length ORF of MYC2 or GFP was ligated into pCAMBIA1301 with 3 Flag-tags in the N-terminal. Each T-DNA was inserted into XS11 using *Agrobacterium*-mediated transformation. The positive lines were screened by hygromycin resistance and GUS staining. In addition, MYC2 overexpression lines were screened by immunoblotting using the monoclonal anti-Flag antibody (Sigma, F1804, 1:5,000 dilution). The *aoc* and *myc2*-deficient lines were generated as previously described (Xu et al. 2021). The *slr1* line was a DELLA loss-of-function mutant, and its background genotype control is the japonica variety, ZH11 (Yang et al. 2012).

RT-qPCR

For rice samples, total RNA was isolated using MiniBEST Plant RNA Extraction Kit (TaKaRa), and 800 ng of total RNA for each sample was reverse transcribed using the HiScript III RT SuperMix (Vazyme). RT-qPCR was performed on the CFX96 Touch (BioRad) using Taq Pro Universal SYBR qPCR Master Mix (Vazyme). The rice *Ubiquitin* mRNA was used as an internal control. For BPH samples, total RNA was isolated by TRIzol. The primers used for detection of target gene transcripts by RT-qPCR are listed in Supplemental

Data Set 2. The BPH β -Actin mRNA was used as an internal control.

Transactivation activity assay

The full-length ORF sequences of MYC2 or SV40 NLS were introduced into pEarlyGate 203 vector (Earley et al. 2006). The 2-kb GA2ox3 and 2-kb GA2ox7 promoter regions were amplified and ligated into pCAMBIA1391z (Cambia), respectively. All constructs were transformed into GV3101 *Agrobacterium*. Leaves of *N. benthamiana* were agroinfiltrated with the indicated reporter and effector constructs at the ratio of 1:1. Two days after infiltration, 3 replicates were collected and incubated in GUS staining buffer (0.5 M phosphate buffer [pH 7.5], 0.5 M EDTA [pH 7.5], 20 mM X-Gluc, and 10% Triton [v/v]) and incubated at 37 °C for 4 h. The chlorophyll of stained leaves was removed by 75% ethanol. For other 8 replicates, samples were harvested and frozen in liquid nitrogen. GUS quantitative assays were performed as described (Li et al. 2015).

EMSA

The probes used in EMSA were designed based on the putative G-box or G-box-like (CANNTG) or T/G-box (AACGTG) motifs from the promoter regions of GA2ox3 and GA2ox7. The mutated probes were synthesized by substituting TTCAA to putative binding motifs. Probe sequences are listed in Supplemental Data Set 2, all of which were labeled with biotin. EMSA was performed using a Chemiluminescent EMSA Kit (Beyotime Biotech) according to manufacturer's instructions. Competition experiments were performed using unlabeled probes as competitors in a 200 \times or 400 \times molar excess.

ChIP assay

Seeds of Flag-tagged MYC2 and GFP plants were sterilized and germinated in 1/2 MS agar medium containing 50 μ g mL⁻¹ Hygromycin B. Five days later, 1.2 g of fresh seedling samples was cut into tiny pieces and crosslinked in 1% (v/v) formaldehyde under vacuum. Chromatin was isolated and sonicated to 200- to 500-bp fragments. The protein–DNA complex was immunoprecipitated by anti-Flag antibody (Sigma, #F1804) bound to Protein A/G Magnetic Beads (Thermo Fisher). The precipitated DNA was analyzed by qPCR. The enrichment of each fragment was calculated by normalizing the amount of a target DNA fragment against a genomic fragment of *Actin* as an internal control. The relative enrichment of each fragment in Flag–GFP precipitated sample was set as “1.” Primers used in ChIP assays are listed in Supplemental Data Set 2.

BPH bioassay

BPH performance on different lines was evaluated by the hatching rate, hatching duration of eggs, and the number of eggs oviposited by adult females. Ten gravid adult females were allowed to feed and oviposit on each plant for 24 h. After removing all of the BPHs, the newly hatched nymphs

were counted every 24 h, until no new nymphs were found. The unhatched eggs from the oviposited leaf sheath were counted under the microscope. Twelve biological replicates were performed.

For plant survival assays, 20 gravid BPH females were allowed to infest each plant, and 10 plants were used for each genotype. The degree of plant damage (ratio of dead leaf number/total leaf number, %) was recorded and photographed after 10 d.

BiFC assay

Full-length ORFs of MYC2, JAZ3, and DELLA without stop codons were cloned into pGTQL1211YN or pGTQL1211YC (gifts from Yuhai Cui, Addgene plasmid #61704 and #61705) and introduced into *Agrobacterium* GV3101 strain. Leaves of 3-wk-old *N. benthamiana* were infiltrated with agrobacterial cells containing the indicated constructs. Two days after incubation, fluorescence was observed by an Olympus confocal microscope (FV3000) with the following parameters: laser wavelength 488 nm: 1%, emission wavelength 509 nm, pinhole 1.00 au/40 μ m, scan speed 4, and detector gain 1,000 (Li et al. 2015).

In vitro pull-down assay

Pull-down assays were performed as described previously (Li et al. 2017); 2 μ g of GST or GST-tagged MYC2 was used to pull-down 2 μ g of HIS-tagged MBP, MBP–JAZ3, or DELLA. The samples were analyzed by SDS/PAGE. After electrophoresis, the gels were stained with Coomassie Brilliant Blue or subjected to immunoblot analysis using an anti-HIS antibody (Abcam, ab18184, 1:5,000 dilution).

Yeast 2-hybrid assay

The full-length ORFs of rice DELLA and 15 JAZs were PCR-amplified and cloned into the GAL4 activation domain (AD) of pGADT7 vector or GAL4 DNA-binding domain (BD) of the pGBKT7 vector, respectively (Clontech). The AD–DELLA and BD–JAZ vector constructs were cotransformed into yeast (*S. cerevisiae*) strain Y2H-Gold according to the manufacturer's instructions. Transformants were selected on SD/-Leu/-Trp plates at 30 °C until colonies appeared. The colonies were transferred into SD/-Leu/-Trp liquid medium overnight. Then the transformant yeasts with AD–DELLA and BD–JAZ were plated on SD/-Leu/-Trp plates and SD/-Ade/-His/-Leu/-Trp containing X- α -gal at 30 °C for 5 d.

Statistical analysis

Student's *t* tests and 1-way ANOVA (Duncan) were performed with Data Processing System (DPS) software (http://www.dpsw.cn/dps_eng/index.html). The summary of statistical analyses is shown in Supplemental Data Set 3.

Accession numbers

The RNA-seq data reported in this paper have been deposited in the Genome Sequence Archive at the BIG Data

Center (<http://bigd.big.ac.cn/gsa>), Beijing Institute of Genomics (BIG), Chinese Academy of Sciences, under accession numbers CRA003587, CRA008166, and CRA008184. Other sequence data from this article could be found in The Rice Annotation Project (RAP) or GenBank under the following accession numbers: Ubiquitin (Os03g0234200); Actin (Os03g0718100); EUI (Os05g0482400); GA3ox2 (Os01g0177400); GA20ox2 (Os01g0883800); GA2ox1 (Os05g0158600); GA2ox2 (Os01g0332200); GA2ox3 (Os01g0757200); GA2ox4 (Os05g0514600); GA2ox5 (Os07g0103500); GA2ox6 (Os04g0522500); GA2ox7 (Os01g0209700); GA2ox8 (Os05g0560900); GA2ox9 (Os02g0630300); GA2ox10 (Os05g0208550); MYC2 (Os10g0575000); JAZ1 (Os04g0653000); JAZ2 (Os07g0153000); JAZ3 (Os08g0428400); JAZ4 (Os09g0401300); JAZ5 (Os04g0395800); JAZ6 (Os03g0402800); JAZ7 (Os07g0615200); JAZ8 (Os09g0439200); JAZ9 (Os03g0180800); JAZ10 (Os03g0181100); JAZ11 (Os03g0180900); JAZ12 (Os10g0392400); JAZ13 (Os10g0391400); JAZ14 (XM_026020773); JAZ15 (Os03g0396500); DELLA (Os03g0707600); GUS (S69414); RRSV P8 (HM125546); β -actin (EU179846); and GUS (S69414).

Acknowledgments

We thank Jing Lv, Jianxiang Wu, Xinjue Wang, Mengyu Liu, Leilei Li, Xuxu Wang, Chuyu Lin, and Zeng Tao for the technical assistance and Shengen Xie for the assistance of BPH rearing. The *slr1* mutant was kindly provided by Prof. Zuhua He (Institute of Plant Physiology and Ecology, Chinese Academy of Sciences).

Author contributions

R.L. designed the research. G.J., J.Q., H.Z., S.L., and R.L. performed the experiments. R.L., G.J., I.T.B., J.G., and Y.L. analyzed the data. R.L., I.T.B., J.G., and G.J. wrote the manuscript.

Supplemental data

The following materials are available in the online version of this article.

Supplemental Figure S1. Growth phenotypes of rice seedlings under different treatments.

Supplemental Figure S2. Detection of RRSV in BPH.

Supplemental Figure S3. The growth phenotypes and GA₃₄ concentrations in AW-treated and control plants.

Supplemental Figure S4. The GA biosynthesis pathway.

Supplemental Figure S5. The effect of GA treatment on BPH-elicited growth restriction.

Supplemental Figure S6. Herbivory-elicited transcript levels of GA3ox2 and GA20ox2 genes in rice.

Supplemental Figure S7. Transcript levels of GA2ox and EUI genes in control and herbivory-elicited rice.

Supplemental Figure S8. The growth phenotypes of GA2ox overexpression and WT plants.

Supplemental Figure S9. Construction of GA2ox mutants.

Supplemental Figure S10. The concentrations of GAs in GA2ox mutants and WT plants.

Supplemental Figure S11. BPH resistance in GA2ox mutants and WT plants.

Supplemental Figure S12. Transcript levels of GA2ox genes in rice under MeJA treatments.

Supplemental Figure S13. Growth phenotypes of *aoc*, *myc2* mutants, and WT plants.

Supplemental Figure S14. Characterization and growth of MYC2 overexpression lines.

Supplemental Figure S15. Phytohormone concentrations in MYC2 overexpression lines and WT plants.

Supplemental Figure S16. Concentrations of bioactive GAs in *myc2* mutants and WT plants under BPH attack.

Supplemental Figure S17. The effects of GA₃ treatment on the growth of MYC2, GA2ox3, and GA2ox7 overexpression lines.

Supplemental Figure S18. The phylogenetic tree analysis of JAZ proteins in Arabidopsis and rice.

Supplemental Figure S19. Protein–protein interaction between DELLA and MYC2.

Supplemental Figure S20. The transcriptional regulation between Arabidopsis MYC2/3 and GA2ox2 gene.

Supplemental Data Set 1. G-box and G-box-like motifs in the promoter of GA2ox3 and GA2ox7.

Supplemental Data Set 2. DNA primers used in this study.

Supplemental Data Set 3. Summary of statistical analyses in this study.

Funding

This work was supported by the National Key Research and Development Program of China (grant no. 2021YFD1401100) (to R.L. and Y.L.), a grant from Max Planck Partner Group Program (to R.L., J.G., and I.T.B.), and the Hundred-Talent Program of Zhejiang University (to R.L.).

Conflict of interest statement. None declared.

References

- Chen Q, Sun J, Zhai Q, Zhou W, Qi L, Xu L, Wang B, Chen R, Jiang H, Qi J, et al. The basic helix-loop-helix transcription factor MYC2 directly represses PLETHORA expression during jasmonate-mediated modulation of the root stem cell niche in Arabidopsis. *Plant Cell* 2011;23(9):3335–3352. <https://doi.org/10.1105/tpc.111.089870>
- Chen S, Zhou Y, Chen Y, Gu J. Fastp: an ultra-fast all-in-one FASTQ preprocessor. *Bioinformatics* 2018;34(17):884–890. <https://doi.org/10.1093/bioinformatics/bty560>
- Chini A, Fonseca S, Fernández G, Adie B, Chico JM, Lorenzo O, García-Casado G, López-Vidriero I, Lozano FM, Ponce MR, et al. The JAZ family of repressors is the missing link in jasmonate signaling. *Nature* 2007;448(7154):666–671. <https://doi.org/10.1038/nature06006>
- Chini A, Monte I, Zamarreno AM, Hamberg M, Lassueur S, Raymond P, Weiss S, Stintzi A, Schaller A, Porzel A, et al. An OPR3-independent pathway uses 4,5-didehydrojasmonate for jasmonate synthesis. *Nat Chem Biol*. 2018;14(2):171–178. <https://doi.org/10.1038/nchembio.2540>

- Coley PD, Bryant JP, Chapin FS.** Resource availability and plant anti-herbivore defense. *Science* 1985;**230**(4728):895–899. <https://doi.org/10.1126/science.230.4728.895>
- de Lucas M, Daviere J-M, Rodriguez-Falcon M, Pontin M, Iglesias-Pedraz JM, Lorrain S, Fankhauser C, Blazquez MA, Titarenko E, Prat S.** A molecular framework for light and gibberellin control of cell elongation. *Nature* 2008;**451**(7177):480–484. <https://doi.org/10.1038/nature06520>
- Deng Y, Ning Y, Yang D-L, Zhai K, Wang G-L, He Z.** Molecular basis of disease resistance and perspectives on breeding strategies for resistance improvement in crops. *Mol Plant*. 2020;**13**(10):1402–1419. <https://doi.org/10.1016/j.molp.2020.09.018>
- Duan J, Yu H, Yuan K, Liao Z, Meng X, Jing Y, Liu G, Chu J, Li J.** Strigolactone promotes cytokinin degradation through transcriptional activation of CYTOKININ OXIDASE/DEHYDROGENASE 9 in rice. *Proc Natl Acad Sci U S A*. 2019;**116**(28):14319–14324. <https://doi.org/10.1073/pnas.1810980116>
- Earley KW, Haag JR, Pontes O, Opper K, Juehne T, Song KM, Pikaard CS.** Gateway-compatible vectors for plant functional genomics and proteomics. *Plant J*. 2006;**45**(4):616–629. <https://doi.org/10.1111/j.1365-3113X.2005.02617.x>
- Erb M, Reymond P.** Molecular interactions between plants and insect herbivores. *Annu Rev Plant Biol*. 2019;**70**:527–557. <https://doi.org/10.1146/annurev-arplant-050718-095910>
- Fernández-Calvo P, Chini A, Fernández-Barbero G, Chico J-M, Gimenez-Ibanez S, Geerinck J, Eeckhout D, Schweizer F, Godoy M, Franco-Zorrilla JM, et al.** The Arabidopsis bHLH transcription factors MYC3 and MYC4 are targets of JAZ repressors and act additively with MYC2 in the activation of jasmonate responses. *Plant Cell* 2011;**23**(2):701–715. <https://doi.org/10.1105/tpc.110.080788>
- Fernández-Milmanda GL, Crocco CD, Reichelt M, Mazza CA, Köellner TG, Zhang T, Cargnel MD, Lichy MZ, Fiorucci A-S, Fankhauser C, et al.** A light-dependent molecular link between competition cues and defence responses in plants. *Nat Plants*. 2020;**6**(3):223–230. <https://doi.org/10.1038/s41477-020-0604-8>
- Fonseca S, Chini A, Hamberg M, Adie B, Porzel A, Kramell R, Miersch O, Wasternack C, Solano R.** (+)-7-iso-Jasmonoyl-L-isoleucine is the endogenous bioactive jasmonate. *Nat Chem Biol*. 2009;**5**(5):344–350. <https://doi.org/10.1038/nchembio.161>
- Fu W, Jin G, Jimenez-Aleman GH, Wang X, Song J, Li S, Lou Y, Li R.** The jasmonic acid-amino acid conjugates JA-Val and JA-Leu are involved in rice resistance to herbivores. *Plant Cell Environ*. 2022;**45**(1):262–272. <https://doi.org/10.1111/pce.14202>
- Gao S, Chu C.** Gibberellin metabolism and signaling: targets for improving agronomic performance of crops. *Plant Cell Physiol*. 2020;**61**(11):1902–1911. <https://doi.org/10.1093/pcp/pcaa104>
- Guo Q, Major IT, Howe GA.** Resolution of growth-defense conflict: mechanistic insights from jasmonate signaling. *Curr Opin Plant Biol*. 2018a;**44**:72–81. <https://doi.org/10.1016/j.pbi.2018.02.009>
- Guo Q, Yoshida Y, Major IT, Wang K, Sugimoto K, Kapali G, Havko NE, Benning C, Howe GA.** JAZ repressors of metabolic defense promote growth and reproductive fitness in *Arabidopsis*. *Proc Natl Acad Sci U S A*. 2018b;**115**(45):E10768–E10777. <https://doi.org/10.1073/pnas.1811828115>
- He J, Chen Q, Xin P, Yuan J, Ma Y, Wang X, Xu M, Chu J, Peters RJ, Wang G.** CYP72A enzymes catalyse 13-hydroxylation of gibberellins. *Nat Plants*. 2019;**5**(10):1057–1065. <https://doi.org/10.1038/s41477-019-0511-z>
- He Z, Webster S, He SY.** Growth-defense trade-offs in plants. *Curr Biol*. 2022;**32**(12):R634–R639. <https://doi.org/10.1016/j.cub.2022.04.070>
- Herms DA, Mattson WJ.** The dilemma of plants: to grow or defend. *Q Rev Biol*. 1992;**67**(3):283–335. <https://doi.org/10.1086/417659>
- Hong G-J, Xue X-Y, Mao Y-B, Wang L-J, Chen X-Y.** Arabidopsis MYC2 interacts with DELLA proteins in regulating sesquiterpene synthase gene expression. *Plant Cell* 2012;**24**(6):2635–2648. <https://doi.org/10.1105/tpc.112.098749>
- Hou X, Lee LY, Xia K, Yen Y, Yu H.** DELLAs modulate jasmonate signaling via competitive binding to JAZs. *Dev Cell*. 2010;**19**(6):884–894. <https://doi.org/10.1016/j.devcel.2010.10.024>
- Hsieh K-T, Chen Y-T, Hu T-J, Lin S-M, Hsieh C-H, Liu S-H, Shiu S-Y, Lo S-F, Wang IW, Tseng C-S, et al.** Comparisons within the rice GA 2-oxidase gene family revealed three dominant paralogs and a functional attenuated gene that led to the identification of four amino acid variants associated with GA deactivation capability. *Rice* (N Y). 2021;**14**(1):70. <https://doi.org/10.1186/s12284-021-00499-4>
- Huot B, Yao J, Montgomery BL, He SY.** Growth-defense tradeoffs in plants: a balancing act to optimize fitness. *Mol Plant*. 2014;**7**(8):1267–1287. <https://doi.org/10.1093/mp/ssu049>
- Kazan K, Manners JM.** MYC2: the master in action. *Mol Plant*. 2013;**6**(3):686–703. <https://doi.org/10.1093/mp/sss128>
- Kim D, Langmead B, Salzberg SL.** HISAT: a fast spliced aligner with low memory requirements. *Nat Methods*. 2015;**12**(4):357–360. <https://doi.org/10.1038/nmeth.3317>
- Li R, Wang M, Wang Y, Schuman MC, Weinhold A, Schafer M, Jimenez-Aleman GH, Barthel A, Baldwin IT.** Flower-specific jasmonate signaling regulates constitutive floral defenses in wild tobacco. *Proc Natl Acad Sci U S A*. 2017;**114**(34):E7205–E7214. <https://doi.org/10.1073/pnas.1703463114>
- Li R, Zhang J, Li J, Zhou G, Wang Q, Bian W, Erb M, Lou Y.** Prioritizing plant defence over growth through WRKY regulation facilitates infestation by non-target herbivores. *Elife* 2015;**4**:e04805. <https://doi.org/10.7554/eLife.04805>
- Li C, Zheng L, Wang X, Hu Z, Zheng Y, Chen Q, Hao X, Xiao X, Wang X, Wang G, et al.** Comprehensive expression analysis of *Arabidopsis* GA2-oxidase genes and their functional insights. *Plant Sci*. 2019;**285**:1–13. <https://doi.org/10.1016/j.plantsci.2019.04.023>
- Liu C, Li D, Li J, Guo Z, Chen Y.** One-pot sample preparation approach for profiling spatial distribution of gibberellins in a single shoot of germinating cereal seeds. *Plant J*. 2019;**99**(5):1014–1024. <https://doi.org/10.1111/tpj.14367>
- Lo S-F, Yang S-Y, Chen K-T, Hsing Y-I, Zeevaart JAD, Chen L-J, Yu S-M.** A novel class of gibberellin 2-oxidases control semidwarfism, tillering, and root development in rice. *Plant Cell* 2008;**20**(10):2603–2618. <https://doi.org/10.1105/tpc.108.060913>
- Ma X, Zhang Q, Zhu Q, Liu W, Chen Y, Qiu R, Wang B, Yang Z, Li H, Lin Y, et al.** A robust CRISPR/Cas9 system for convenient, high-efficiency multiplex genome editing in monocot and dicot plants. *Mol Plant*. 2015;**8**(8):1274–1284. <https://doi.org/10.1016/j.molp.2015.04.007>
- Machado RAR, Baldwin IT, Erb M.** Herbivory-induced jasmonates constrain plant sugar accumulation and growth by antagonizing gibberellin signaling and not by promoting secondary metabolite production. *New Phytol*. 2017;**215**(2):803–812. <https://doi.org/10.1111/nph.14597>
- McKey D.** The distribution of secondary compounds within plants. In *Herbivores: their interaction with secondary plant metabolites*. 1979:55–134.
- Panda S, Jozwiak A, Sonawane PD, Szymanski J, Kazachkova Y, Vainer A, Kilambi HV, Almekias-Siegl E, Dikaya V, Bocobza S, et al.** Steroidal alkaloids defence metabolism and plant growth are modulated by the joint action of gibberellin and jasmonate signalling. *New Phytol*. 2022;**233**(3):1220–1237. <https://doi.org/10.1111/nph.17845>
- Pertea M, Pertea GM, Antonescu CM, Chang T-C, Mendell JT, Salzberg SL.** Stringtie enables improved reconstruction of a transcriptome from RNA-seq reads. *Nat Biotechnol*. 2015;**33**(3):290–295. <https://doi.org/10.1038/nbt.3122>
- Rhoades DF, Cates RG.** Toward a general theory of plant antiherbivore chemistry. In *Biochemical interaction between plants and insects* (Springer). 1976:168–213. https://doi.org/10.1007/978-1-4684-2646-5_4

- Sheard LB, Tan X, Mao H, Withers J, Ben-Nissan G, Hinds TR, Kobayashi Y, Hsu F-F, Sharon M, Browse J, et al.** Jasmonate perception by inositol-phosphate-potentiated COI1-JAZ co-receptor. *Nature* 2010;**468**(7322):400–405. <https://doi.org/10.1038/nature09430>
- Sun TP.** The molecular mechanism and evolution of the GA-GID1-DELLA signaling module in plants. *Curr Biol.* 2011;**21**(9):R338–R345. <https://doi.org/10.1016/j.cub.2011.02.036>
- Thines B, Katsir L, Melotto M, Niu Y, Mandaokar A, Liu G, Nomura K, He SY, Howe GA, Browse J.** JAZ repressor proteins are targets of the SCFCO11 complex during jasmonate signalling. *Nature* 2007;**448**(7154):661–665. <https://doi.org/10.1038/nature05960>
- Tong H, Xiao Y, Liu D, Gao S, Liu L, Yin Y, Jin Y, Qian Q, Chu C.** Brassinosteroid regulates cell elongation by modulating gibberellin metabolism in rice. *Plant Cell.* 2014;**26**(11):4376–4393. <http://doi.org/10.1105/tpc.114.132092>
- Uji Y, Taniguchi S, Tamaoki D, Shishido H, Akimitsu K, Gomi K.** Overexpression of OsMYC2 results in the up-regulation of early JA-responsive genes and bacterial blight resistance in rice. *Plant Cell Physiol.* 2016;**57**(9):1814–1827. <https://doi.org/10.1093/pcp/pcw101>
- Wang X, Chen Y, Liu S, Fu W, Zhuang Y, Xu J, Lou Y, Baldwin IT, Li R.** Functional dissection of rice jasmonate receptors involved in development and defense. *New Phytol.* 2023;**238**(5):2144–2158. <https://doi.org/10.1111/nph.18860>
- Wasternack C, Feussner I.** The oxylipin pathways: biochemistry and function. *Annu Rev Plant Biol.* 2018;**69**:363–386. <https://doi.org/10.1146/annurev-arplant-042817-040440>
- Wasternack C, Hause B.** Jasmonates: biosynthesis, perception, signal transduction and action in plant stress response, growth and development. An update to the 2007 review in *Annals of Botany.* *Ann Bot.* 2013;**111**(6):1021–1058. <https://doi.org/10.1093/aob/mct067>
- Xu J, Wang X, Zu H, Zeng X, Baldwin IT, Lou Y, Li R.** Molecular dissection of rice phytohormone signaling involved in resistance to a piercing-sucking herbivore. *New Phytol.* 2021;**230**(4):1639–1652. <https://doi.org/10.1111/nph.17251>
- Yamaguchi S.** Gibberellin metabolism and its regulation. *Annu Rev Plant Biol.* 2008;**59**:225–251. <https://doi.org/10.1146/annurev-arplant.59.032607.092804>
- Yang T-H, Lenglet-Hilfiker A, Stolz S, Glauser G, Farmer EE.** Jasmonate precursor biosynthetic enzymes LOX3 and LOX4 control wound-response growth restriction. *Plant Physiol.* 2020;**184**(2):1172–1180. <https://doi.org/10.1104/pp.20.00471>
- Yang D-L, Yao J, Mei C-S, Tong X-H, Zeng L-J, Li Q, Xiao L-T, Sun T-P, Li J, Deng X-W, et al.** Plant hormone jasmonate prioritizes defense over growth by interfering with gibberellin signaling cascade. *Proc Natl Acad Sci U S A.* 2012;**109**(19):E1192–E1200. <https://doi.org/10.1073/pnas.1201616109>
- Zander M, Lewsey MG, Clark NM, Yin L, Bartlett A, Guzman JPS, Hann E, Langford AE, Jow B, Wise A, et al.** Integrated multi-omics framework of the plant response to jasmonic acid. *Nat Plants.* 2020;**6**(3):290–302. <https://doi.org/10.1038/s41477-020-0605-7>
- Zheng X-Y, Spivey NW, Zeng W, Liu P-P, Fu ZQ, Klessig DF, He SY, Dong X.** Coronatine promotes *Pseudomonas syringae* virulence in plants by activating a signaling cascade that inhibits salicylic acid accumulation. *Cell Host Microbe.* 2012;**11**(6):587–596. <https://doi.org/10.1016/j.chom.2012.04.014>
- Zhu YY, Nomura T, Xu YH, Zhang YY, Peng Y, Mao BZ, Hanada A, Zhou HC, Wang RX, Li PJ, et al.** ELONGATED UPPERMOST INTERNODE encodes a cytochrome P450 monooxygenase that epoxidizes gibberellins in a novel deactivation reaction in rice. *Plant Cell* 2006;**18**(2):442–456. <https://doi.org/10.1105/tpc.105.038455>